Available online at www.sciencedirect.com

ScienceDirect

Ceramics International 40 (2014) 417–422

CERAMICS INTERNATIONAL

www.elsevier.com/locate/ceramint

Sol–gel deposition of fluorine-doped tin oxide glasses for dye sensitized solar cells

Ian Y.Y. Bu*

Department of Microelectronics Engineering, National Kaohsiung Marine University, Kaohsiung City, Taiwan, Republic of China

Received 13 April 2013; received in revised form 8 June 2013; accepted 10 June 2013
Available online 15 June 2013

Abstract

Thin films of fluorine-doped tin-oxide (FTO) were prepared by a sol–gel process using the combination of $SnCl_2 \cdot H_2O$, NH_4F and isopropanol. The effects of annealing temperature on structural, electrical and optical properties of FTO were studied. It was found that films annealed at temperatures above 500 °C exhibit resistivity of around 30 Ω/sq with an optical transparency up to 90%, which is comparable with commercially available FTO coated glasses. A dye-sensitized solar cell was fabricated with the optimized thin film and yielded power conversion efficiency ~1.58%.

Keywords: A. Sol—gel processes; B. Nanocomposites; C. Electrical properties; E. Electrodes

1. Introduction

Recently, dye-sensitized solar cells (DSSCs) have attracted considerable attention due to their potential to lower the overall cost of solar cells [1–4]. Although power conversion efficiency greater than 12% has been achieved by DSSCs [5], however, the overall cost still remains high [6]. Past strategies for cost reduction have focused on three main areas. (1) Enhancing photo-anodes through adapting nanostructured materials (TiO_2 [3,7], ZnO [8,9] and SnO [10,11]); (2) replacing Pt counter electrodes with cheaper alternative nanomaterials (carbon nanotubes [12], carbon black [13] and cobalt sulfide [14]) or (3) developing higher performance dyes to replace the expensive Ru-based N719 dye [15,16]. Amid all the attentions on these related issues, the cost of FTO glasses has rarely been addressed. Break down cost analysis on DSSC productions have revealed that FTO coated glass substrate constitutes around 40% of the material costs [17]. Although a wide range of transparent conductive oxides (TCO), such as ITO [18] and AZO [19], have been investigated for DSSCs, FTO is preferred due to its superior chemical stability and greater tolerance during photo-anode annealing processes [20–22]. Currently, the commercially available FTOs are deposited by using the spray pyrolysis technique [23,24]. The primary costs associated with spray pyrolysis are the equipment expenditure, which is difficult to eliminate. Therefore, in order to reduce the overall production costs, alternative deposition techniques must be adopted [25]. The sol–gel process deposition is particularly attractive because it offers precise control of film composition, requires only simple equipment set-up and offers large-area deposition. Generally, sol–gel derived thin films are strongly affected by the deposition conditions such as sintering temperature, impurity incorporation, precursor ageing, pH and molar concentration. Previous studies on sol–gel derived FTO thin films have utilized combinations of $SnCl_2$, HF and alcohol [26]. To our best knowledge, there are very few studies on the sol–gel synthesis of FTO using NH_4F [25]. Furthermore, there is lack of studies on DSSCs fabrication using sol–gel derived FTO [27]. The main difference between the present study and Ray's study [25] is the deposition technique. Ray employed a dip-coating deposition method that coated both sides of the substrate, whereas, the films investigated in the present study were deposited by using a spin coating technique, which offers better thickness control and uniformity. In this study, the effects of temperature on the structure and optoelectronic properties of sol–gel derived FTO thin films were investigated. The derived FTO thin films were characterized through scanning

*Tel./fax: +8869 7250 6900.
E-mail address: ianbu@hotmail.com

0272-8842/$ - see front matter © 2013 Elsevier Ltd and Techna Group S.r.l. All rights reserved.
http://dx.doi.org/10.1016/j.ceramint.2013.06.017

electron microscope (SEM), X-ray diffraction (XRD) and the Hall effect measurements. For each sample, the Hall effect measurements were performed five times. By using the optimized FTO films, DSSCs were constructed and tested.

2. Experimental

All chemicals used in this study were of reagent grade and used without further purification. First, Corning Eagle 2000 glasses were cleaned using ultrasonic agitation in acetone, isopropanol, deionized water and were blown dry using an N_2 gun purge. Then 0.7 M of $SnCl_2 \cdot H_2O$ in IPA was mixed for 2 h at room temperature. Fluorine doping was achieved by adding NH_4F (F:Sn 50:1) into the pre-mixed solution. Previous studies [26] have revealed that fluorine-rich precursor are required to obtain sufficient doping through the sol–gel method due to non-vacuum deposition condition. The mixed FTO solution precursor was left to age for 48 h, which gave it a gel-like consistency. To deposit a uniform coating on the substrate, the precursor sol was spin coated onto the glass substrates at 3000 rpm for 30 s. Subsequently, the coated substrate was pre-heated at 250 °C and post sintered between 400 and 550 °C, respectively.

The morphology of the deposited FTO thin films was examined by using an FEI quanta 400F environmental scanning electron microscopy (SEM). Chemical composition was determined by energy dispersive spectroscopy equipped within the SEM. A Siemens D5000 X-ray diffractometer with Cu Kα radiation was used to obtain the crystalline orientation and grain size of the thin films. Hall effect measurements in a Van der Pauw configuration were used to determine the electrical conductivity type, resistivity and mobility. Optical transmittance and the Tauc gap were determined using a UV–vis NIR (Hitachi U-4100). DSSCs were fabricated by sandwiching a dye-sensitized TiO_2 photo-anode and a Pt counter electrode between two pieces of FTO coated glass substrates. Specifically, the TiO_2 photo-anode was prepared by using the doctor-blade method through a 3 M tape mask and heated to 450 °C in order to sinter and remove organic compounds. This coating process was repeated 3 times to yield a thickness of around 15 μm. Then the TiO_2 nanoparticle layer was immersed into a 0.3 M solution of N719 dye (Eversolar) mixed in dry ethanol at 60 °C for 24 h. Catalytic counter electrode was formed by sputtering 15 nm of Pt. The sandwich structure was partially sealed by hot compressing a Suryn sheet between the photo-anode and counter electrode at 125 °C. A mixture of 0.12 M I_2, 0.1 M LiI and 0.5 M tertbutylpyridine in 3-methoxypropionitrile was used as the electrolyte. This solution was injected through pre-drilled holes and fully sealed with Suryn thin film. Solar cell Illuminated current–voltage characteristics were measured by a solar simulator (Science tech).

3. Results and discussions

Fig. 1(a), (b), (c) and (d) shows the SEM image of the synthesized FTO thin films at different temperatures. The inserts show the same set of SEM images at lower magnifications. Clearly, at lower magnifications, it can be observed that

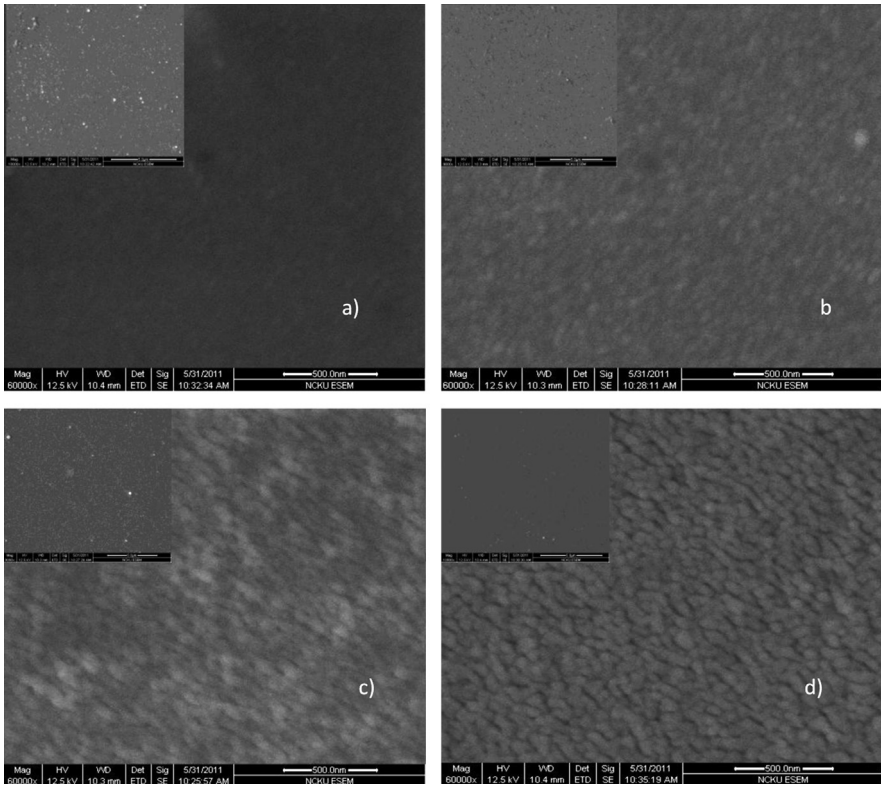

Fig. 1. SEM image of the sol–gel derived SnO_2:F films deposited at (a) 400, (b) 450, (c) 500 and (d) 550 °C. Insert shows the same SEM images at lower magnification (5 μm).

all the derived FTO thin films appear to be smooth and without cracks and voids. It is interesting to notice that a few particles appeared on the film surfaces, which is caused by particle agglomeration.

Upon closer examination of the SEM images at higher magnification levels, it can be observed that the FTO thin films are composed of uniform particles with diameters of around 50～80 nm. These SEM images indicate that the film structure are influenced by the post sintering temperature with more apparent grain formation as the sintering temperature increases. Generally, commercially available FTO consists of well-connected grains with average diameters of around 200 nm. Since the commercially available FTO glasses are synthesized by spray pyrolysis of Sn and F compounds at around 500 °C, the difference is caused by deposition techniques, not by sintering temperature. The formation of smaller grains from this study suggests a greater amount of grain boundary in the sol–gel derived FTO films, which could lead to increased charge trapping.

Fig. 2(a) shows the XRD diffraction patterns of sol–gel derived FTO on glass substrates at different post sintering temperatures, 400, 450, 500 and 550 °C, respectively. The peaks (110), (101), (211) and (220) can be indexed to a tetragonal SnO_2 crystal structure. Clearly, the increase in annealing temperature resulted in enhanced crystallization of the films. All the deposited FTO thin films exhibited a strong preference to (110) plane, which correlates well with previous studies [26]. Fig. 2(b) presents the variations in the Full Width at Half Maximum (FWHM) of the investigated films with respect to the sintering temperature. It can be observed that the FWHM for the (100) plane of the thin films increases with higher sintering temperatures. The grain size was obtained through the Scherrer's formula

$$d = \frac{0.9\lambda}{B\cos\vartheta_B}$$

where λ is the X-ray wavelength (1.54 Å), θ_B is the Bragg diffraction angle and $\boldsymbol{B}$ is the FWHM of θ_B. As expected, an increase in post-sintering temperature results in the formation of larger grains due to thermally activated crystallization. The increase in grain size and decrease in the FWHM also indicate enhancement in the film crystallinity.

One of the key parameters of FTO is its sheet resistance because it can affect electron transfer and eventually the solar cell power conversion efficiency. The sheet resistance of the thin-films was determined by using the four-probe method. Fig. 3 shows the variations in sheet resistances as a function of the post annealing temperature. Clearly, the sheet resistance reduces as the sintering temperature increases due to enhanced crystallization of the thin-film, which reaches the minimum at around 30 Ω/cm. The typical sheet resistance of commercially available FTO coated glass is around 15 Ω/cm, which is around half of the sheet resistance value of the investigated thin film. As compared with intrinsic tin oxide, the fluorine doping of tin oxide reduced the particle size, increased the grain boundaries and decreased the resistance of the films. Fig. 3 indicates that the sheet resistance initially decreases with

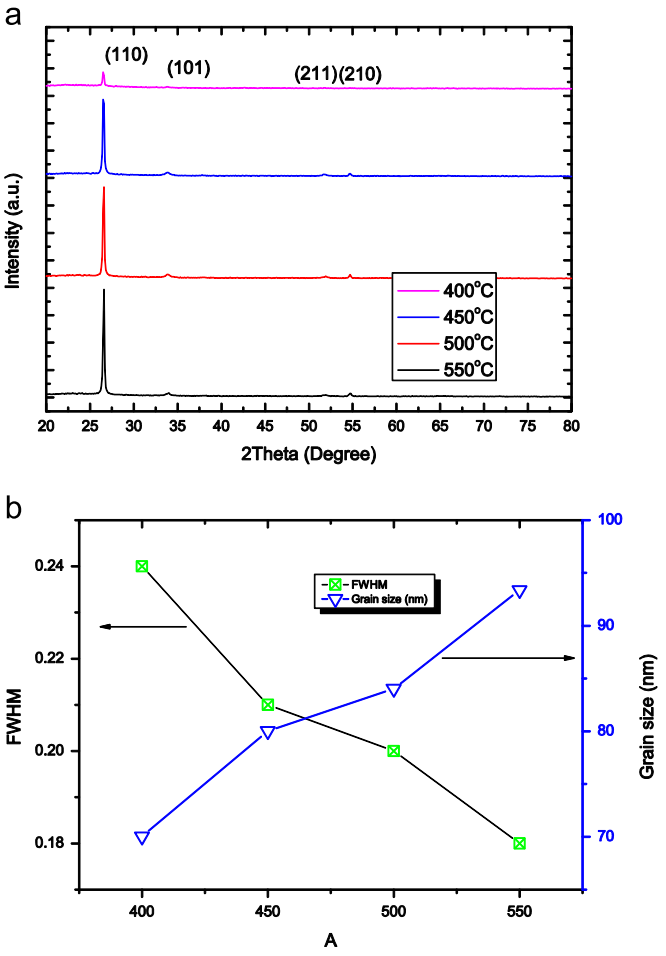

Fig. 2. (a) XRD patterns of the sol–gel derived SnO_2:F films and (b) the extracted FWHM and grain size from the Scherrer's formula.

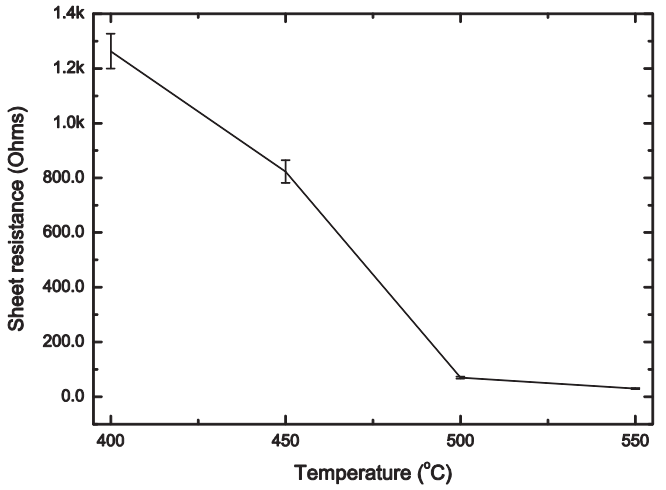

Fig. 3. Effects of sintering temperature on sheet resistance of sol–gel derived SnO_2:F.

increasing annealing temperature until at around 500 °C, at which point the tendency reverses and increases again. This reversal in sheet resistances originates from the fluorine out-diffusion of the film, which is replaced by oxygen from the

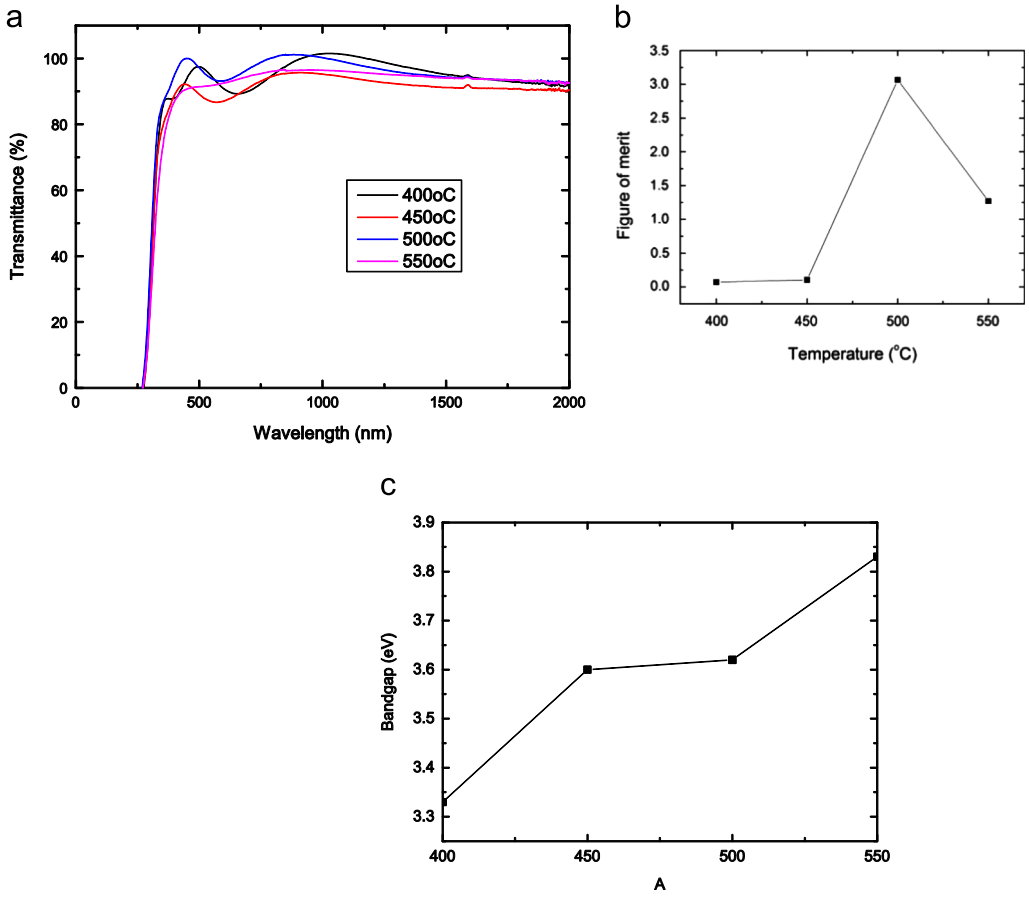

Fig. 4. shows the effects of annealing temperature on (a) optical transmittance against wavelength, (b) figure of merit and (c) extracted Tauc gap.

atmosphere [26]. The oxygen-compensation process shifts the overall film composition towards stoichiometric tin oxide and as a result, leads to decrease in carrier concentration and increase in sheet resistance. Furthermore, films sintered at excessive temperatures are susceptible to impurity metal ion diffusion from the glass substrate. Once incorporated into the films, these impurities can introduce structural defects, counter dope the sample and reduce carrier mobility [28].

Fig. 4 shows the transmittance of the deposited FTO thin films as a function of the annealing temperatures. All the synthesized FTO films exhibit a good degree of transparency, with an average transmittance of around 89%, 86%, 92% and 89% for films deposited at 400, 450, 500 and 550 °C, respectively. Typically, commercially available FTO glasses are deposited on thick glass substrates (2.5–6 mm) and possess transparency of around 88%. In terms of DSSCs processing, thicker glass substrates are heavier, suffer from non-uniformity issues, and require longer annealing time. Furthermore, thicker films tend to absorb more light and degrade optical transparency.

Quantitative figure of merit data (resistance/transmittance at 550 nm) can be obtained by combining the extracted electrical data (Fig. 3) with the transmittance data (Fig. 4(a)). Fig. 4(b) shows the calculated "figure of merit" as a function of sintering temperature. As expected, films annealed at higher temperatures tend to have the higher figure of merits due to the reduction in the sheet resistivity, with the best film obtained at around 500 °C.

The optical band gap (Tauc Gap) can be obtained by analyzing the absorption edge and applying the Tauc model

$$(\alpha h\nu) = A(h\nu - E_g)^{1/2}$$

where α is the absorption coefficient, h is the Planck's constant, ν is frequency of vibration, A is a constant and E_g is the band gap. The optical band gap of FTO films prepared by using the sol–gel method was determined by extrapolating the slope from the plot in Fig. 4(a) and by the plotting in Fig. 4(c). Fig. 4 (c) shows the changes in band gap with sintering temperature. The band gap increases with increasing sintering temperature from 3.33 eV to 3.83 eV, which is close to the reported band gap for SnO_2 3.3–4.0 eV [26]. This increase in band-gap can be attributed to the Burstein–Moss shift; the absorption edge shifts towards higher energy with an increase in carrier density. Based on the Hall effect measurement, the carrier density of the FTO films increases from 2.1×10^{18} to 5.3×10^{19} cm^{-3} as sintering temperature increases from 400 to 550 °C (not shown).

DSSCs were fabricated by using the FTO (sintered at 500 °C) developed in this study. Fig. 5 shows the photovoltaic performance of the DSSCs fabricated using the sol–gel deposited FTO glass. Key process parameters extracted from

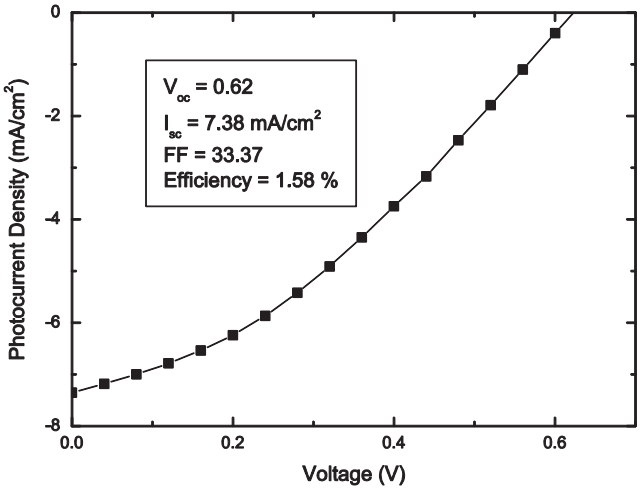

Fig. 5. *J–V* characteristics of the assembled DSSCs using sol–gel derived FTO glass.

the illuminated *J–V* characteristics include the open circuit (V_{OC})∼0.62, short circuit current density (J_{SC})∼7.38 mA/cm**,** fill factor∼33.37 and an overall power conversion efficiency of around 1.58%. By comparing with the typical DSSCs fabricated in our laboratory, there is a reduction in both the J_{sc} and FF but similar V_{OC}. Previous experiments have revealed that the V_{OC} is related to the metal oxide (in our case TiO_2) and the electrolyte used in DSSCs assembly. Since the TiO_2 and electrolyte were not altered during this study, the V_{OC} was not expected to change. However, the FF and J_{sc} are related to a combination of factors that include defect related recombination at the TiO_2/FTO interface, resistivity of TCOs and counter electrodes. It is believed that the degradation occurring in both of these parameters is due to a combination of all these factors but with high resistivity of the sol–gel derived FTO most probable cause. Although the photovoltaic performance of sol–gel derived FTO glasses have not yet matched the commercially available FTO glasses, the results presented in this study demonstrates its potential in DSSCs applications. It is well-known that sol–gel derived thin films are highly influenced by the process parameters (temperature, the pH of the precursor, solvent, etc.). Therefore, further optimization of the FTO thin film is expected to hold the key to improving the performance of DSSCs.

4. Conclusion

Highly transparent and conductive FTO thin film has been obtained by the sol–gel technique. Effects of sintering temperature on the the optoelectronic and structural properties of sol–gel deposited FTO thin films were investigated. It was found that highly transparent and conductive FTO thin film can be achieved through the use of the sol–gel technique with best electrical performance obtained with films deposited at 500 °C. SEM images revealed that the derived films consisted of small grains with diameters ranging from 60 to 100 nm. From the XRD patterns, it was found that increasing sintering temperature resulted in tetragonal SnO_2 films with higher crystallinity and with a preference toward (110) orientation. The optimized FTO thin film was used to fabricate DSSCs and was characterized for its photovoltaic performances. A DSSCs solar cell with an overall power conversion efficiency∼1.58% was obtained. Although the fabricated DSSCs using sol–gel derived FTO do not match commercially available FTOs, this study demonstrated their potential for future research.

References

[1] H.-G. Bang, J.-K. Chung, R.-Y. Jung, S.-Y. Park, Effect of acetic acid in TiO_2 paste on the performance of dye-sensitized solar cells, Ceramics International 38 (2012) S511–S515.
[2] J.H. Yum, E. Baranoff, F. Kessler, T. Moehl, S. Ahmad, T. Bessho, A. Marchioro, E. Ghadiri, J.E. Moser, C. Yi, A cobalt complex redox shuttle for dye-sensitized solar cells with high open-circuit potentials, Nature Communications 3 (2012) 631.
[3] B. O'regan, M. Gratzel, A low-cost, high-efficiency solar cell based on dye-sensitized colloidal TiO_2 films, Nature 353 (6346) (1991) 737–740.
[4] N. Saelim, R. Magaraphan, T. Sreethawong, TiO_2 modified natural clay semiconductor as a potential electrode for natural dye-sensitized solar cell, Ceramics International 37 (2) (2011) 659–663.
[5] A. Yella, H.W. Lee, H.N. Tsao, C. Yi, A.K. Chandiran, M. K. Nazeeruddin, E.W.G. Diau, C.Y. Yeh, S.M. Zakeeruddin, M. Grätzel, Porphyrin-sensitized solar cells with cobalt (II/III)-based redox electrolyte exceed 12 percent efficiency, Science 334 (6056) (2011) 629–634.
[6] J. Kroon, N. Bakker, H. Smit, P. Liska, K. Thampi, P. Wang, S. Zakeeruddin, M. Grätzel, A. Hinsch, S. Hore, Nanocrystalline dye-sensitized solar cells having maximum performance, Progress in Photovoltaics: Research and Applications 15 (1) (2007) 1–18.
[7] A. Bakhshayesh, M. Mohammadi, The improvement of electron transport rate of TiO_2 dye-sensitized solar cells using mixed nanostructures with different phase compositions, Ceramics International (2013).
[8] K. Keis, C. Bauer, G. Boschloo, A. Hagfeldt, K. Westermark, H. Rensmo, H. Siegbahn, Nanostructured ZnO electrodes for dye-sensitized solar cell applications, Journal of Photochemistry and Photobiology A: Chemistry 148 (1–3) (2002) 57–64.
[9] Y. Lin, J. Yang, Y. Meng, Nanostructured ZnO thin films by SDS-assisted electrodeposition for dye-sensitized solar cell applications, Ceramics International (2012).
[10] S. Chappel, A. Zaban, Nanoporous SnO_2 electrodes for dye-sensitized solar cells: improved cell performance by the synthesis of 18 nm SnO_2 colloids, Solar Energy Materials and Solar Cells 71 (2) (2002) 141–152.
[11] N. Cai, J. Cho, Low temperature processed SnO_2 films using aqueous precursor solutions, Ceramics International 39 (2012) 143–151.
[12] K. Suzuki, M. Yamaguchi, M. Kumagai, S. Yanagida, Application of carbon nanotubes to counter electrodes of dye-sensitized solar cells, Chemistry Letters 32 (1) (2003) 28–29.
[13] A. Kay, M. Grätzel, Low cost photovoltaic modules based on dye sensitized nanocrystalline titanium dioxide and carbon powder, Solar Energy Materials and Solar Cells 44 (1) (1996) 99–117.
[14] M. Wang, A.M. Anghel, B.T. Marsan, N.-L. Cevey Ha, N. Pootrakulchote, S.M. Zakeeruddin, M. Gratzel, CoS supersedes Pt as efficient electrocatalyst for triiodide reduction in dye-sensitized solar cells, Journal of the American Chemical Society 131 (44) (2009) 15976–15977.
[15] T. Maeda, Y. Hamamura, K. Miyanaga, N. Shima, S. Yagi, H. Nakazumi, Near-infrared absorbing squarylium dyes with linearly extended π-conjugated structure for dye-sensitized solar cell applications, Organic Letters 18 (2011) 5994–5997.
[16] D.P. Hagberg, J.H. Yum, H.J. Lee, F. De Angelis, T. Marinado, K. M. Karlsson, R. Humphry-Baker, L. Sun, A. Hagfeldt, M. Grätzel, Molecular engineering of organic sensitizers for dye-sensitized solar cell applications, Journal of the American Chemical Society 130 (19) (2008) 6259–6266.

[17] M.Y. Yen, C.Y. Yen, S.H. Liao, M.C. Hsiao, C.C. Weng, Y.F. Lin, C.C. M. Ma, M.C. Tsai, A. Su, K.K. Ho, A novel carbon-based nanocomposite plate as a counter electrode for dye-sensitized solar cells, Composites Science and Technology 69 (13) (2009) 2193–2197.
[18] W. Hong, Y. Xu, G. Lu, C. Li, G. Shi, Transparent graphene/PEDOT–PSS composite films as counter electrodes of dye-sensitized solar cells, Electrochemistry Communications 10 (10) (2008) 1555–1558.
[19] S. Sutthana, N. Hongsith, S. Choopun, AZO/Ag/AZO multilayer films prepared by DC magnetron sputtering for dye-sensitized solar cell application, Current Applied Physics 10 (3) (2010) 813–816.
[20] Z. Zhou, R. Cui, Q. Pang, Y. Wang, F. Meng, T. Sun, Z. Ding, X. Yu, Preparation of indium tin oxide films and doped tin oxide films by an ultrasonic spray CVD process, Applied Surface Science 172 (3–4) (2001) 245–252.
[21] M. Takai, D. Bollmann, K. Haberger, Maskless patterning of indium tin oxide layer for flat panel displays by diode-pumped Nd:YLF laser irradiation, Applied Physics Letters 64 (19) (1994) 2560–2562.
[22] S.I. Noh, H.-J. Ahn, D.-H. Riu, Photovoltaic property dependence of dye-sensitized solar cells on sheet resistance of FTO substrate deposited via spray pyrolysis, Ceramics International 38 (2012) 3735–3739.
[23] E. Shanthi, A. Banerjee, V. Dutta, K. Chopra, Electrical and optical properties of tin oxide films doped with F and (Sb+F), Journal of Applied Physics 53 (3) (1982) 1615–1621.
[24] A. Rakhshani, Y. Makdisi, H. Ramazaniyan, Electronic and optical properties of fluorine-doped tin oxide films, Journal of Applied Physics 83 (2) (1998) 1049–1057.
[25] S.C. Ray, M.K. Karanjai, D. DasGupta, Tin dioxide based transparent semiconducting films deposited by the dip-coating technique, Surface and Coatings Technology 102 (1) (1998) 73–80.
[26] A. Banerjee, S. Kundoo, P. Saha, K. Chattopadhyay, Synthesis and characterization of nano-crystalline fluorine-doped tin oxide thin films by sol–gel method, Journal of Sol–Gel Science and Technology 28 (1) (2003) 105–110.
[27] H.-M. Kwon, D.-W. Han, D.-J. Kwak, Y.-M. Sung, Preparation of nanoporous F-doped tin dioxide films for TCO-less dye-sensitized solar cells application, Current Applied Physics 10 (2) (2010) S172–S175.
[28] D. Zhang, L. Tao, Z. Deng, J. Zhang, L. Chen, Surface morphologies and properties of pure and antimony-doped tin oxide films derived by sol–gel dip-coating processing, Materials Chemistry and Physics 100 (2) (2006) 275–280.